Quasiparticle band structures of the antiferromagnetic transition-metal oxides MnO, FeO, CoO, and NiO

C. Rödl, F. Fuchs, J. Furthmüller, and F. Bechstedt

Institut für Festkörpertheorie und -optik, Friedrich-Schiller-Universität and European Theoretical Spectroscopy Facility (ETSF), Max-Wien-Platz 1, 07743 Jena, Germany

(Received 4 December 2008; revised manuscript received 6 March 2009; published 8 June 2009)

Quasiparticle (QP) band structures for antiferromagnetic MnO, FeO, CoO, and NiO are calculated within the *GW* approximation using wave functions and energy eigenvalues obtained from a generalized Kohn-Sham scheme with the nonlocal exchange-correlation functional HSE03 which accounts for screened exchange. This improved starting point for the exchange-correlation self-energy leads to an efficient solution of the QP equation and remedies the failure of the *GW* approach on top of (semi)local Kohn-Sham schemes for these materials. The resulting band gaps and densities of states (DOS) show good agreement with measurements for all four oxides. The fit of the results from GGA+U calculations with an additional scissors shift Δ to these benchmark QP DOS allows to reproduce the QP DOS widely.

DOI: 10.1103/PhysRevB.79.235114 PACS number(s): 71.15.Qe, 71.20.Ps, 71.27.+a, 71.45.Gm

I. INTRODUCTION

The electronic structure of the late transition-metal (TM) monoxides MnO, FeO, CoO, and NiO, which show antiferromagnetic behavior below their respective Néel temperatures, has been discussed intensively for many years. Originally, these oxides, which crystallize in rocksalt structure in the paramagnetic phase, were thought to be examples of prototypical Mott insulators.[1] The Mott-Hubbard theory asserts that electron correlation characterized by the *d-d* intraatomic Coulomb energy U is much larger than the 3*d* bandwidth, thereby giving rise to a gap between the filled and empty *d* states. Later, Terakura *et al.*[2] stated that the TM oxides are not Mott insulators but conventional band-gap insulators with a fundamental gap created by exchange and crystal-field splittings,[3] i.e., due to the long-range magnetic ordering.[2] X-ray photoemission spectroscopy (XPS) and bremsstrahlung isochromat spectroscopy (BIS) experiments (see, e.g., Refs. 4 and 5) are not conclusive and both pictures are brought up for their interpretation. The experimentally observed fundamental gaps are usually considerably smaller than the predicted Mott-Hubbard U.[6] Hence, the TM oxides lie in the intermediate region of the Zaanen-Sawatzky-Allen phase diagram[7] or can be termed charge-transfer insulators.[6]

It is a widely held belief that conventional band theory cannot be applied to systems like the late TM oxides because the resulting band gaps and magnetic moments are considerably smaller than experimental values.[8] Even the quasiparticle (QP) theory with an exchange-correlation (XC) self-energy in Hedin's *GW* approximation[9]—the tool of choice for the determination of electronic excitation properties from first principles for systems with weak or moderate Coulomb correlation, such as *sp* semiconductors—is questioned to be applicable and suggested to be replaced[8] by or combined[10] with the dynamical mean-field theory (DMFT). However, DMFT requires as a starting point the spin-polarized density-functional theory (DFT) within a local-density approximation (LDA) or a generalized-gradient approximation (GGA) in combination with an empirical Mott-Hubbard parameter U, the so-called LDA+U (GGA+U) method.[11]

On the other hand, based on LDA/GGA electronic structures, the QP method has already been used to describe the band structures of MnO and NiO with reasonable but varying gaps.[12–14] For antiferromagnetic FeO and CoO with a metallic ground state within LDA or GGA,[3] i.e., TM oxides with seemingly stronger electron correlation, the conventional QP method fails. Their electronic structure is even less clear from the theoretical point of view as well as experimentally.

For these reasons, we calculate QP band structures and densities of states (DOS) for the antiferromagnetic TM oxides within Hedin's *GW* approach following a recently developed improved procedure:[15] instead of starting from an LDA or GGA band structure, one-particle wave functions and energy eigenvalues are calculated applying the spatially nonlocal XC potential derived from the HSE03 functional.[16,17] By construction, the HSE03 functional features a nonlocal screened-exchange contribution similar to the *GW* self-energy itself. Thus, the corresponding generalized Kohn-Sham (gKS) equation, which is solved self-consistently, can be interpreted as a QP equation with a reasonable zeroth approximation to the XC self-energy. It has been shown for a variety of materials[15] that this improved starting point justifies the calculation of QP corrections within the first-order perturbation-theory approach G_0W_0 for materials where LDA(GGA)+G_0W_0 computations fail. Especially localized orbitals, as the shallow *d* states, are described much better from the very beginning.

In order to understand the effects of electron correlation in the improved QP picture more deeply, we consider the HSE03+G_0W_0 results as a benchmark and attempt to reproduce them within the computationally less expensive and conceptionally easier GGA+U scheme. The value for the on-site interaction U is obtained by mimicking the HSE03 +G_0W_0 valence-band DOS, especially the relative position of the occupied TM 3*d* states with t_{2g} and e_g symmetry and, hence, the band ordering. An additional scissors shift Δ representing the excitation aspect is required to bring also the conduction states of the GGA+U approach in acceptable accordance with the HSE03+G_0W_0 results.

The paper is organized as follows: In Sec. II we summarize the computational details of the performed calculations.

QP band structures, band gaps, and DOS within the HSE03 $+G_0W_0$ approach are presented and discussed in Sec. III. Further, we compare the obtained DOS to GGA$+U+\Delta$ calculations in Sec. IV.

II. COMPUTATIONAL DETAILS

All computations have been performed using the Vienna *ab initio* simulation package (VASP).[18,19] The 4*s* and 3*d* electrons of the TM atoms as well as the oxygen 2*s* and 2*p* electrons are treated as valence states. The electronic wave functions are described using a basis set of plane waves with kinetic energies up to 315 eV (MnO), 325 eV (NiO), or 400 eV (FeO and CoO), whereas the projector-augmented wave (PAW) method is employed to set up the wave functions in the core regions. For the GGA calculations the Perdew-Wang parametrization[20] of the XC functional is used. Intermediate spin polarization is described by the interpolation scheme of von Barth and Hedin.[21]

In all computations the Brillouin zone is sampled by a mesh of $8\times8\times8$ **k** points which includes the Γ point for all considered materials. The inverse dielectric function and the matrix elements of the self-energy are determined from the HSE03 eigenvalues and wave functions without any adjustable parameters.[22] Thereby, the screening function is evaluated taking into account 150 energy bands.

The GGA$+U$ calculations are based on the rotationally invariant scheme of Dudarev *et al.*,[23] where only the difference of the on-site interaction and the exchange parameter $U-J$ enters the total energy. Consequently, all values for U used here have to be considered as effective values $U-J$.

The lattice constants for the rocksalt TM oxides in the antiferromagnetic ordering AFII (stacking of ferromagnetic planes in [111] direction) are taken from experiments:[24–26] 8.863 Å (MnO), 8.666 Å (FeO), 8.499 Å (CoO), and 8.341 Å (NiO). Small rhombohedral or tetragonal distortions, as evident from x-ray or neutron diffraction measurements[24,26] below the Néel temperature, have been neglected.

III. QUASIPARTICLE BAND STRUCTURES

A. HSE03$+G_0W_0$ approach

Early attempts[3] describing the TM oxides in a band-structure approach within the LDA proved that it is possible to obtain a finite fundamental gap for antiferromagnetic MnO and NiO. The reasons for the gap opening are the exchange splitting between the spin-up and spin-down *d* orbitals in the case of MnO and the crystal-field splitting between the minority-spin channel t_{2g} and e_g states for NiO. Nevertheless, such an approach fails for CoO and FeO. For these oxides, the energy gap should occur within the minority-channel t_{2g} states but a local approach to XC is not able to open a gap within these states. It is well known that also the semilocal GGA does not improve the band gaps significantly above the LDA values in comparison to the large gaps known from experiment (see, e.g., Ref. 27 or Table II).

Principally, DFT as a ground-state theory should not give proper QP energy gaps, which are one-particle excitation properties. A well-established method to describe excitation properties of semiconductors and insulators, such as photoemission spectra, consists in starting from a Kohn-Sham (KS) band structure and adding QP corrections in the *GW* approach.[9,38] To this end, the QP equation has to be solved, what should be done self-consistently, in principle. Although some approaches to self-consistency exist,[14,39] these schemes are computationally extremely demanding. The prevailing way to calculate QP shifts called G_0W_0 is the solution of the QP equation in first-order perturbation theory, which yields reasonable gaps for many materials with a slight tendency to gap underestimation.[15] Applying this approach to MnO and NiO results in energy gaps which are by far too low compared to the experimental findings (cf. Refs. 13 and 14 and Table II). The reason for the failure of this approximation consists in the invalidity of the perturbational treatment of the QP equation. The perturbation-theory approach is only justified if the subjacent KS gap has already the order of the experimental gaps. Indeed, the gap corrections, which are presumed to be small, amount to more than 80% for MnO and NiO (see Table II), which is clearly beyond the capabilities of perturbation theory.

The failure of GGA$+G_0W_0$ for the TM oxides is now identified not to result from the QP theory itself, but from the inappropriateness of the subjacent KS approach, which is based on a (semi)local treatment of XC. To cure this problem, we use the nonlocal screened hybrid functional HSE03 (Refs. 16 and 17) to describe XC in the gKS equation. This functional is especially appealing, since it already contains a statically screened nonlocal exchange contribution which is an important part of the *GW* self-energy[38] and in large part responsible for the gap opening. With this in mind, one can consider the use of the HSE03 functional as a step toward self-consistency in the solution of the QP equation.

Another drawback of the LDA/GGA can be remedied using the HSE03 functional: local treatments of XC are designed to describe systems with spatially slowly varying electron density. Despite the fact that these approximations are quite successful for many *sp* semiconductors, they tend to fail, if localized states such as shallow *d* levels are involved. More precisely, they underestimate the degree of localization of these states. This should result also in a significant change in the wave functions used to determine the QP corrections. The degree of localization can be demonstrated by examination of integral quantities such as the local magnetic moments at the TM sites (see Table I): in GGA we obtain results in accordance with previous calculations.[27] As it is well known, the computed values underestimate the experimental findings, especially in the case of CoO where the orbital contribution to the magnetic moment is argued to be comparably large. However, taking spatial nonlocality into account within the HSE03 approach enhances the local magnetic moments toward the experimental values.

B. Dielectric constants and fundamental gaps

The values of the fundamental gaps for the series of oxides from MnO to NiO are summarized in Table II. In contrast to the GGA results, we find insulating behavior for all

TABLE I. Local magnetic moments m in μ_B for the antiferromagnetic TM oxides.

	MnO	FeO	CoO	NiO
GGA	4.3	3.4	2.4	1.3
HSE03	4.5	3.6	2.7	1.6
GGA+U	4.5	3.6	2.6	1.5
Experiment	4.58[a]	3.32[b], 4.2[c]	3.35[d], 3.8[b,e], 3.98[f]	1.90[a,b]

[a]Reference 24.
[b]Reference 40.
[c]Reference 41.
[d]Reference 42.
[e]Reference 43.
[f]Reference 26.

four oxides applying the HSE03 treatment of XC in the gKS equation—i.e., also for FeO and CoO, which are metals in GGA, a gap opens. In comparison to the GGA gaps the HSE03 values are significantly larger and prove to be already of the same order of magnitude as the experimental findings (cf. Table II). This has also been observed by Marsman *et al.*[44] Thus, the obtained band structures are promising candidates for a QP calculation.

The formation of QPs is governed by the screening reaction of the electron system, i.e., by the inverse frequency- and wave-vector-dependent dielectric matrix.[9,38] In the static and long-wavelength limit the screening properties can be characterized by the microscopic static electronic dielectric constant $\varepsilon_\infty^{\mathrm{mic}}$. However, the inversion of the dielectric matrix yields the so-called macroscopic constants $\varepsilon_\infty^{\mathrm{mac}}$, where local-field effects are included according to the Adler-Wiser relation.[45,46] In Table III we compare the dielectric constants obtained by evaluating the dielectric matrix in random-phase approximation (RPA) utilizing the GGA or HSE03 energy eigenvalues and eigenfunctions, respectively. Due to the strong gap underestimation in GGA, the absorption onset lies at much too low energies and the dielectric constants are by far overestimated. This becomes particularly obvious for NiO yielding a value of 25.3 in comparison to the experimental result of 5.7. The same behavior is observed for MnO, although the difference of 8.4 compared to 4.95 is much smaller. Usually, the RPA dielectric constants in GGA match well with experimental findings for many semiconductors,[15,39] but the strong gap underestimation in the TM oxides compared to conventional semiconductors causes this remarkable overshoot. On the contrary, the HSE03 dielectric constants are close to the experimental results (see Table III) with a slight tendency to too low values, a trend also observed for conventional semiconductors.[15] The smallness of the difference between $\varepsilon_\infty^{\mathrm{mic}}$ and $\varepsilon_\infty^{\mathrm{mac}}$ in Table III demonstrates the weak influence of local-field effects on the dielectric properties of the antiferromagnetic TM oxides. Recently, this has also been observed for the optical absorption spectrum of MnO.[49]

TABLE III. Microscopic ($\varepsilon_\infty^{\mathrm{mic}}$) and macroscopic ($\varepsilon_\infty^{\mathrm{mac}}$) static electronic dielectric constants in GGA and HSE03 as well as experimental values (Refs. 47 and 48).

	MnO	FeO	CoO	NiO
$\varepsilon_\infty^{\mathrm{mic}}$ (GGA)	8.6			25.5
$\varepsilon_\infty^{\mathrm{mac}}$ (GGA)	8.4			25.3
$\varepsilon_\infty^{\mathrm{mic}}$ (HSE03)	4.1	4.5	4.4	4.7
$\varepsilon_\infty^{\mathrm{mac}}$ (HSE03)	4.0	4.4	4.3	4.5
ε_∞ (experiment)	4.95		5.3	5.7

TABLE II. Indirect (ind.) and direct (dir.) energy gaps E_g calculated within the GGA+G_0W_0 and HSE03+G_0W_0 approaches in comparison to the lowest gaps E_g^{exp} from photoemission (photoem.), conductivity (cond.), or optical absorption (opt. abs.) measurements. The fit parameters for the effective on-site Coulomb interaction U and the scissors shift Δ of the GGA+U+Δ approach are also listed. All values are given in eV.

	MnO		FeO		CoO		NiO	
	ind.	dir.	ind.	dir.	ind.	dir.	ind.	dir.
E_g (GGA)	0.7	1.1	0.0		0.0		0.6	0.8
E_g (GGA+G_0W_0)	1.7	2.1					1.1	1.4
E_g (HSE03)	2.6	3.2	2.1	2.2	3.2	4.0	4.1	4.5
E_g (HSE03+G_0W_0)	3.4	4.0	2.2	2.3	3.4	4.5	4.7	5.2
E_g^{exp} (photoem.)	3.9 ± 0.4 [a]				2.5 ± 0.3 [b]		4.3[c]	
E_g^{exp} (cond.)	3.8…4.2 [d]				3.6 ± 0.5 [e]		3.7[f]	
E_g^{exp} (opt. abs.)	3.6…3.8 [g]		2.4[h]		2.8[i], 5.43[j]		3.7[k], 3.87[j]	
U	2.0		3.0		3.0		3.0	
Δ	3.0		1.5		2.5		2.0	

[a]Reference 4.
[b]Reference 28.
[c]Reference 29.
[d]Reference 30.
[e]Reference 31.
[f]Reference 32.
[g]Reference 33.
[h]Reference 34.
[i]Derived from Fig. 1 of Ref. 35.
[j]Reference 36.
[k]Reference 37.

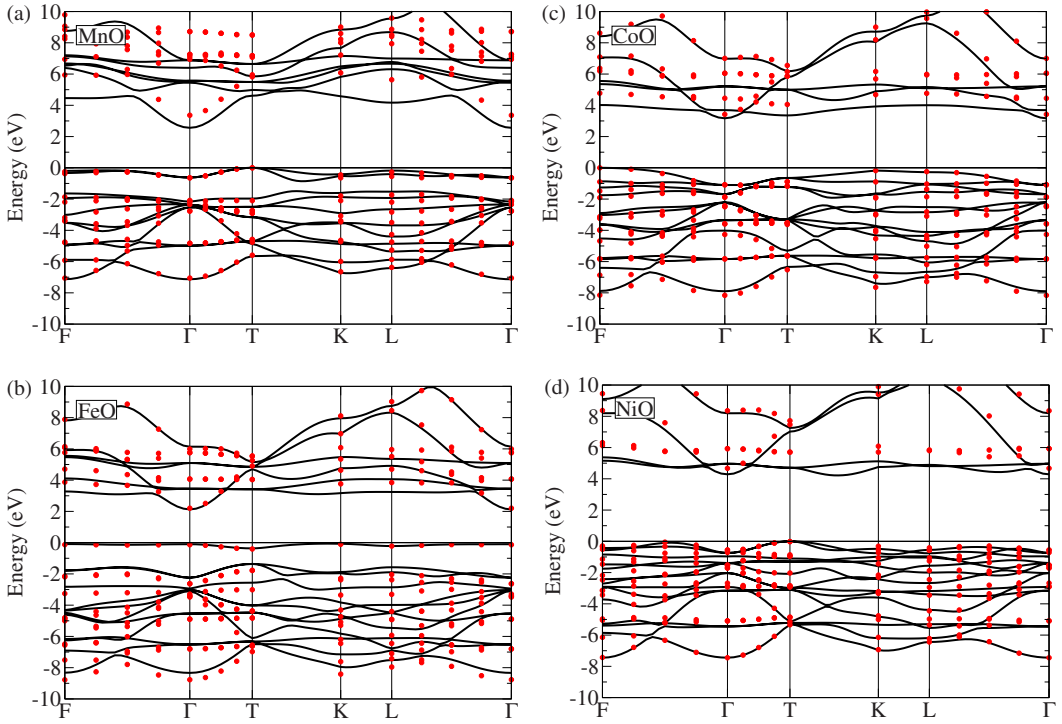

FIG. 1. (Color online) QP band structures for MnO (a), FeO (b), CoO (c), and NiO (d). Red dots denote the QP energies obtained within G_0W_0 on top of the HSE03 calculation (black lines). The VBM is used as energy zero for both the HSE03 as well as the QP bands.

Solving the QP equation with the improved starting point of HSE03 eigenvalues and wave functions opens the fundamental gaps even further. In principle, the calculated indirect QP gaps should compare with the results from XPS/BIS-derived values, while a detailed analysis of the optical gaps requires a further discussion concerning optically allowed or forbidden transitions[50] and excitonic effects.[49] However, also the combination of XPS and BIS results to obtain gaps is difficult for these materials due to the Fermi-level alignment and the extremely low DOS at the onset of the conduction bands (see Sec. III D).

For MnO the inclusion of QP shifts yields a substantial gap opening of 0.8 eV. The calculated gap matches experimental findings from photoemission, conductivity, and optical absorption measurements. Also for NiO a comparably large gap opening occurs, resulting in an indirect gap of 4.7 eV, somewhat larger than the photoemission gap of 4.3 eV. In the case of FeO, the HSE03 already seems to give a good estimate for the gap, since the additional opening of 0.1 eV due to the solution of the QP equation is quite small. For comparison with measurements, only the gap derived from optical absorption of the nonstoichiometric wüstite phase is available, but this value is still in good agreement with our results. For CoO the experimental situation is quite unclear, since the derived gaps span a large energy range hampering comparison. A more detailed discussion of the whole one-particle spectra in comparison to photoemission data follows in Sec. III D.

C. Band structures and QP shifts

In Fig. 1 the QP band structures of the TM oxides in the HSE03+G_0W_0 approach are plotted. The band structure of MnO including the rhombohedral distortion of the unit cell has been published previously.[49] All studied materials are indirect semiconductors. In MnO and NiO, the valence-band maximum (VBM) is located at the T point, while it can be found at F in CoO. In FeO the topmost occupied band is almost dispersionless. The highest valence bands of all four oxides are dominated by TM 3d states with some admixture of O 2p character. Consequently, they are strongly localized and show little dispersion. The conduction-band minimum (CBM) can be found at Γ in all studied materials. The parabola-shaped lowest conduction band exhibits a comparably strong dispersion and features TM 4s character at Γ. Above this s-like band, the nearly dispersionless unoccupied TM 3d states can be found.

A detailed analysis of the QP shifts with respect to the gKS starting point is interesting for the understanding of electronic excitations in systems with localized d electrons. In Fig. 2 we compare the QP shifts on top of the GGA and HSE03 band structures. In order to analyze the effects of the QP approach for the TM oxides in more detail, the shifts in Fig. 2 are classified with respect to their orbital character, i.e., they are labeled as d if the contribution of d states exceeds 50% and as sp otherwise. First, one observes that the semicore O 2s states shift by approximately 1 eV (MnO) or 0.5 eV (NiO) if GW corrections are applied on top of a GGA band structure, whereas they remain almost unshifted for all four TM oxides if the HSE03 functional is used in the subjacent gKS equation. Hence, one can conclude that an HSE03 treatment of such deep-lying localized states is superior to the GGA. Also the spreading of the QP shifts for the valence-band O 2p states is reduced for the HSE03 functional compared to GGA. Another feature that is also visible

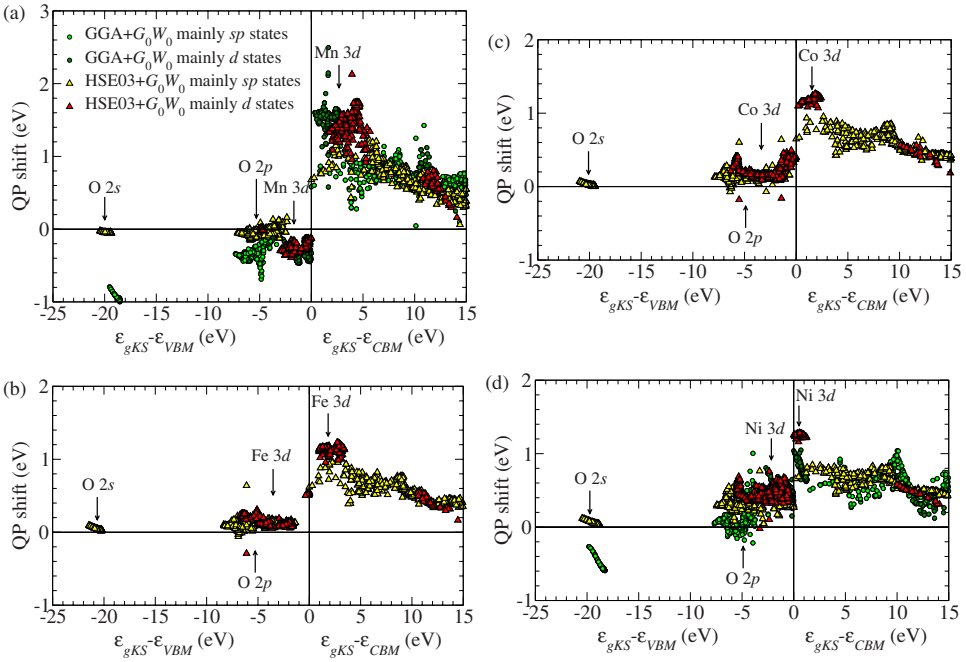

FIG. 2. (Color online) QP shifts obtained in the G_0W_0 approach with respect to the subjacent (g)KS eigenvalues ε_{gKS} for MnO (a), FeO (b), CoO (c), and NiO (d). Circles denote shifts with respect to the GGA calculation for states which show dominating (more than 50%) *d* character (dark green) or mainly *sp* character (light green). Triangles represent shifts based on the HSE03 approach for states with predominantly *d* character (red) or *sp* character (yellow). The VBM or CBM are used as energy zeros for the valence-band or conduction-band states, respectively.

in the band structures is the strong upward shift of the unoccupied *d* states compared to the empty *sp* states. Thus, the additional gap opening proves to be quite small, whereas the position of the *d* peaks in the conduction-band DOS is significantly modified by the QP effects. On the whole, the shifts are strongest in MnO, which is in accordance with the expectations, since the difference between the HSE03 and the experimental gap is largest for this material. Altogether, the QP shifts are much more character dependent than the ones observed for *sp* semiconductors.[15]

D. Densities of states

In Fig. 3 we compare the QP DOS of the four antiferromagnetic TM oxides within the HSE03+G_0W_0 approach with experimental XPS and BIS spectra. Additionally, the DOS have been projected onto the TM orbitals with t_{2g} and e_g symmetry, respectively. For comparison, it has to be noted that in the XPS spectra the photoionization cross sections for the oxygen *p* states are much lower than those for the TM *d* states. Hence, the partial DOS of the latter is predominantly probed by the experiments. Good agreement of the main

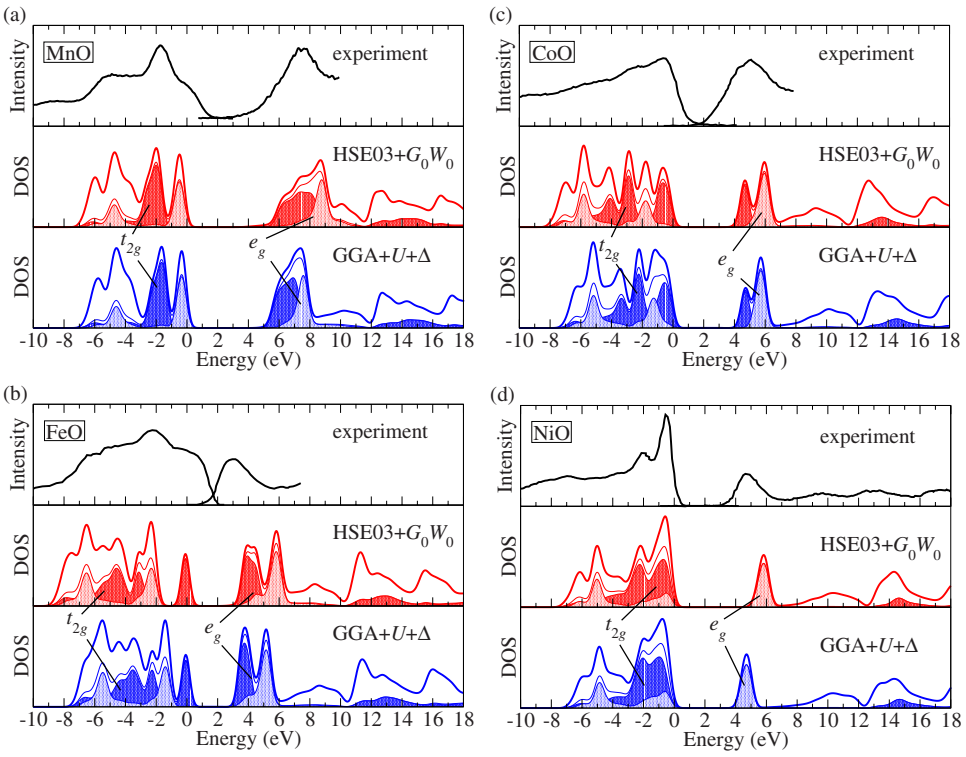

FIG. 3. (Color online) DOS for MnO (a), FeO (b), CoO (c), and NiO (d) in the HSE03+G_0W_0 approach (middle panel) compared with experimental XPS and BIS spectra (Refs. 4, 28, 29, and 51) (upper panel). In the lower panel the DOS obtained by using the GGA+U method with an additional scissors shift Δ is shown. In the calculated spectra the contributions of the TM *d* states (thin solid line) with t_{2g} (dark shaded) and e_g (light shaded) symmetry to the total DOS (thick solid line) are also indicated. For better comparison the computed DOS are broadened by a Gaussian with 0.6 eV full width at half maximum. The top of the valence bands is taken as energy zero.

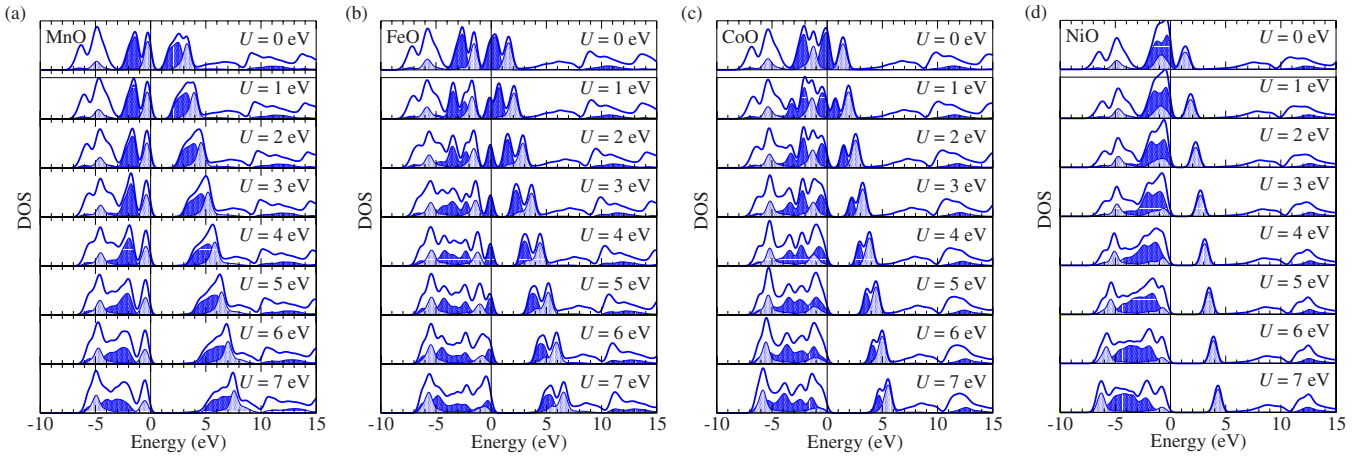

FIG. 4. (Color online) DOS (solid line) for MnO (a), FeO (b), CoO (c), and NiO (d) calculated with different values for U in the GGA+U scheme *without* an additional scissors shift. The contributions of the TM 3d states with t_{2g} (dark shaded) and e_g (light shaded) symmetry are shown as well. A Gaussian broadening of 0.6 eV full width at half maximum is applied to all curves and the top of the valence bands is taken as energy zero.

peaks in the calculated DOS is found with respect to the prominent peaks in the experimental spectra.

For MnO (see also Ref. 49) the occupied as well as unoccupied 3d states match peaks or shoulders in the measurements. Especially the high-energy shoulder and the main peak of the XPS spectrum can be identified as the t_{2g} and e_g peaks of the occupied d states. The main feature of the BIS spectrum, a very broad peak between 6 and 9 eV, is due to the unoccupied d states and agrees with our calculated DOS.

In the case of NiO, the double-peak structure of the valence-band DOS is well reproduced, while the unoccupied 3d e_g states lie about 1 eV too high in energy. The same overestimation of the energetical position of the unoccupied e_g bands has been also obtained by Faleev *et al.*[14] in their self-consistent *GW* calculation. Such an effect might be due to the neglect of vertex corrections in the XC self-energy.[9]

The agreement between our findings and the quite featureless measured spectra of CoO, which exhibit a large experimental broadening, proves to be good. The partial DOS of the valence d states shows the same decrease going to lower energies as the XPS spectrum. The corresponding BIS spectrum exhibits just one extremely broad peak which matches the position of the double peak caused by the unoccupied t_{2g} and e_g states. The photoemission gap of 2.5 ± 0.3 eV derived by Elp *et al.*[28] from their experimental spectra [see Fig. 3(c)] is lower than our calculated value. This might be a consequence of the large experimental broadening (1.0 eV for the XPS and 0.8 eV for the BIS) inherent in the measured spectra.

For FeO we obtain the peak positions in the valence-band region in agreement with the XPS spectrum. The broad shoulder near the VBM is caused by the very flat Fe 3d t_{2g} band [see Fig. 1(b)]. Both t_{2g} and e_g states contribute to the most pronounced peak in the XPS spectrum. Also the plateau-like behavior at lower energies can be explained. However, the unoccupied states seem to lie at too high energies in comparison to the BIS spectrum. Unfortunately, Zimmermann *et al.*[51] did not derive a value for the fundamental gap from their experimental data. Nevertheless, optical measurements[34] indicate—in accordance with our results—a band gap of 2.4 eV, which is much larger than the gap one would estimate from the alignment of the XPS and BIS spectra in Ref. 51.

As it is visible from the band structures in Fig. 1 and the DOS in Fig. 3, the valence-band states are dominated by flat TM 3d and dispersive oxygen 2p bands. In the region around the VBM the contribution of the latter is minor, but not negligible. In the energy range above the CBM, on the other hand, unoccupied TM 3d bands as well as states that show predominantly TM 4s symmetry at Γ can be found. The lowest conduction band features a significant dispersion in the surroundings of the Brillouin-zone center. This fact should be taken into consideration in the derivation of gaps from XPS/BIS spectra, since the s states, due to their very low DOS in comparison to the d states, are almost invisible in BIS measurements.

IV. COMPARISON TO THE GGA+U+Δ APPROACH

The observation of a gap opening in the HSE03 approach for the oxides CoO and FeO asks for a more detailed discussion in terms of strong correlation on the 3d shell and its relation to the calculation of one-particle excitation spectra. The most pronounced effects occur for the minority-spin t_{2g} states, whose occupation increases gradually from MnO to NiO. GGA already yields a gap for MnO and NiO, since they exhibit completely empty or filled minority-channel t_{2g} bands, respectively. On the contrary, the Fermi level lies within these states in CoO and FeO, where the t_{2g} orbitals are only partially occupied. The improved treatment of XC in the HSE03+G_0W_0 approach splits the t_{2g} bands in accordance with their occupancies, due to the included screened exchange. Correspondingly, the energy ranges below the VBM and above the CBM exhibit large t_{2g} contributions.

In order to shed light on the electron interaction in the 3d shell, the DOS has also been calculated within the GGA+U method. The results are depicted in Fig. 4. The U parameter can be interpreted as a spatially nonlocal interaction af-

fecting the strongly localized TM *d* states. In the approach of Dudarev *et al.*[23] the thereby introduced additional term in the XC potential possesses the form of an intra-atomic orbital-dependent screened-exchange-like interaction. Now, the question arises how the value of the parameter U has to be determined. By varying this parameter, it is possible to shift the occupied *d* states in the DOS downward in energy by several eV, whereas the empty *d* states are shifted upward as it is visible in Fig. 4. Choosing large values of U, as typically suggested in literature (see, e.g., Refs. 6 and 11), results in a complete reordering of the excitation spectrum, which is inconsistent with the observations from XPS measurements (cf. Fig. 3). More precisely, the occupied *d* states are shifted downward in energy with respect to the GGA. In that case, the energy range below the VBM is mainly determined by O $2p$ states, which is clearly in contradiction to experimental findings. Moreover, such a procedure does not cause the fundamental gap to open sufficiently to obtain agreement with experimental results for all of the studied compounds. This is due to the admixture of O $2p$ states to the highest valence bands and the *s*-like conduction band forming the CBM. Both are only indirectly and, therefore, hardly influenced by the on-site interaction.

On the contrary, a small U—lying in the same order of magnitude as the bandwidth of the minority-channel t_{2g} bands—leads to valence-band DOS in good agreement with the findings from experiment and our HSE03+G_0W_0 calculations. Therefore, we choose a value for U (cf. Table II) which allows us to mimic the DOS for the valence bands as obtained from the HSE03+G_0W_0 approach. Applying this procedure restricts us to an accuracy of ~ 1 eV in the determination of U. Getting the correct position of the conduction bands requires an additional parameter, the scissors shift Δ, which is a consequence of the excitation of QPs. The scissors shift, as the simplest approach to QP corrections, allows to bring also the position of the conduction states, at least the ones derived from TM *d* states, in accordance with the experimental and HSE03+G_0W_0 results. The overall agreement between the HSE03+G_0W_0 and the GGA+U+Δ DOS is surprisingly good (see Fig. 3). The relative position and weight of the t_{2g} and e_g bands in GGA+U+Δ matches the results of the more sophisticated computation very well. Nevertheless, one has to keep in mind that this procedure, though computationally very cheap, cannot replace a proper *ab initio* QP calculation, since it contains two fitting parameters U and Δ.

The need for both parameters, U and Δ, to reproduce the QP electronic structure of the HSE03+G_0W_0 approach suggests that the on-site interaction U, typically used to characterize strongly correlated systems, as well as the pure excitation aspects, as described by the scissors shift Δ, have to be taken into account likewise to describe the one-particle excitation spectra of the TM oxides accurately.

V. SUMMARY AND CONCLUSIONS

We have studied the QP band structures of the transition-metal oxides MnO, FeO, CoO, and NiO in their antiferromagnetic phase. Going one step beyond the usual method of calculating QP corrections in G_0W_0 on top of an LDA/GGA band structure, we start from the nonlocal hybrid functional HSE03. The HSE03 functional features a screened-exchange contribution and can, therefore, be regarded as a first step toward self-consistency in the QP equation, since such a screened exchange is a major contribution to the *GW* self-energy. Furthermore, the nonlocality of the HSE03 functional accounts much better for the strong localization of the TM $3d$ states and the nonlocality of the electron-electron interaction than a local treatment of XC in the KS equation.

Within this approach we obtain band structures which clearly indicate insulators with fundamental gaps matching the experimental findings. Moreover, we are able to calculate DOS in good agreement with XPS and BIS measurements. Hence, the failure of predicting correct band structures is attributed not to the *GW* approach itself, but to its perturbative treatment starting from (semi)local XC functionals.

For a better understanding of the underlying mechanisms which open the gaps, we have approximated the energy eigenvalues and eigenfunctions by those of a GGA+U calculation with an additional scissors shift Δ. U and Δ have been adjusted to reproduce the more sophisticated HSE03+G_0W_0 DOS. The resulting values for U and Δ, which are of the same order of magnitude, are interpreted to indicate that both aspects, strong Coulomb repulsion on the $3d$ shell as well as excitation-dominated gap opening, have to be taken into account simultaneously. Such a GGA+U+Δ approach proves to be able to reproduce the experimental as well as the QP spectra, but contains two fit parameters. These parameters have to be determined by means of an *ab initio* QP calculation.

ACKNOWLEDGMENTS

We acknowledge financial support from the European Community within the I3 project ETSF (GA No. 211956) and the Deutsche Forschungsgemeinschaft (Project Nos. Be 1346/18-2 and Be 1346/20-1).

[1] B. H. Brandow, Adv. Phys. **26**, 651 (1977).
[2] K. Terakura, A. R. Williams, T. Oguchi, and J. Kübler, Phys. Rev. Lett. **52**, 1830 (1984).
[3] K. Terakura, T. Oguchi, A. R. Williams, and J. Kübler, Phys. Rev. B **30**, 4734 (1984).
[4] J. van Elp, R. H. Potze, H. Eskes, R. Berger, and G. A. Sawatzky, Phys. Rev. B **44**, 1530 (1991).
[5] S. Hüfner, P. Steiner, I. Sander, F. Reinert, and H. Schmitt, Z. Phys. B: Condens. Matter **86**, 207 (1992).
[6] J. Zaanen and G. A. Sawatzky, J. Solid State Chem. **88**, 8 (1990).
[7] J. Zaanen, G. A. Sawatzky, and J. W. Allen, Phys. Rev. Lett. **55**,

418 (1985).
[8] X. Ren, I. Leonov, G. Keller, M. Kollar, I. Nekrasov, and D. Vollhardt, Phys. Rev. B **74**, 195114 (2006).
[9] W. G. Aulbur, L. Jönsson, and J. W. Wilkins, in *Solid State Physics: Advances in Research and Applications*, edited by H. Ehrenreich and F. Spaepen (Academic Press, San Diego, 2000), Vol. 54, p. 1.
[10] S. Biermann, F. Aryasetiawan, and A. Georges, Phys. Rev. Lett. **90**, 086402 (2003).
[11] V. I. Anisimov, J. Zaanen, and O. K. Andersen, Phys. Rev. B **44**, 943 (1991).
[12] S. Massidda, A. Continenza, M. Posternak, and A. Baldereschi, Phys. Rev. Lett. **74**, 2323 (1995).
[13] F. Aryasetiawan and O. Gunnarsson, Phys. Rev. Lett. **74**, 3221 (1995).
[14] S. V. Faleev, M. van Schilfgaarde, and T. Kotani, Phys. Rev. Lett. **93**, 126406 (2004).
[15] F. Fuchs, J. Furthmüller, F. Bechstedt, M. Shishkin, and G. Kresse, Phys. Rev. B **76**, 115109 (2007).
[16] J. Heyd, G. E. Scuseria, and M. Ernzerhof, J. Chem. Phys. **118**, 8207 (2003).
[17] A. V. Krukau, O. A. Vydrov, A. F. Izmaylov, and G. E. Scuseria, J. Chem. Phys. **125**, 224106 (2006).
[18] G. Kresse and J. Furthmüller, Comput. Mater. Sci. **6**, 15 (1996).
[19] G. Kresse and D. Joubert, Phys. Rev. B **59**, 1758 (1999).
[20] J. P. Perdew and Y. Wang, Phys. Rev. B **45**, 13244 (1992).
[21] U. von Barth and L. Hedin, J. Phys. C **5**, 1629 (1972).
[22] M. Shishkin and G. Kresse, Phys. Rev. B **74**, 035101 (2006).
[23] S. L. Dudarev, G. A. Botton, S. Y. Savrasov, C. J. Humphreys, and A. P. Sutton, Phys. Rev. B **57**, 1505 (1998).
[24] A. K. Cheetham and D. A. O. Hope, Phys. Rev. B **27**, 6964 (1983).
[25] B. Hentschel, Z. Naturforsch. A **25**, 1996 (1970).
[26] W. Jauch, M. Reehuis, H. J. Bleif, F. Kubanek, and P. Pattison, Phys. Rev. B **64**, 052102 (2001).
[27] P. Dufek, P. Blaha, V. Sliwko, and K. Schwarz, Phys. Rev. B **49**, 10170 (1994).
[28] J. van Elp, J. L. Wieland, H. Eskes, P. Kuiper, G. A. Sawatzky, F. M. F. de Groot, and T. S. Turner, Phys. Rev. B **44**, 6090 (1991).
[29] G. A. Sawatzky and J. W. Allen, Phys. Rev. Lett. **53**, 2339 (1984).
[30] I. A. Drabkin, L. T. Emel'yanova, R. N. Iskenderov, and Y. M. Ksendzov, Fiz. Tverd. Tela (Leningrad) **10**, 3082 (1968).
[31] M. Gvishi and D. S. Tannhauser, J. Phys. Chem. Solids **33**, 893 (1972).
[32] Y. M. Ksendzov and I. A. Drabkin, Fiz. Tverd. Tela (Leningrad) **7**, 1884 (1965).
[33] R. N. Iskenderov, I. A. Drabkin, L. T. Emel'yanova, and Y. M. Ksendzov, Fiz. Tverd. Tela (Leningrad) **10**, 2573 (1968).
[34] H. K. Bowen, D. Adler, and B. H. Auker, J. Solid State Chem. **12**, 355 (1975).
[35] G. W. Pratt, Jr. and R. Coelho, Phys. Rev. **116**, 281 (1959).
[36] T. D. Kang, H. S. Lee, and H. Lee, J. Korean Phys. Soc. **50**, 632 (2007).
[37] R. J. Powell and W. E. Spicer, Phys. Rev. B **2**, 2182 (1970).
[38] L. Hedin, Phys. Rev. **139**, A796 (1965).
[39] M. Shishkin and G. Kresse, Phys. Rev. B **75**, 235102 (2007).
[40] W. L. Roth, Phys. Rev. **110**, 1333 (1958).
[41] P. D. Battle and A. K. Cheetham, J. Phys. C **12**, 337 (1979).
[42] D. C. Khan and R. A. Erickson, Phys. Rev. B **1**, 2243 (1970).
[43] D. Herrmann-Ronzaud, P. Burlet, and J. Rossat-Mignod, J. Phys. C **11**, 2123 (1978).
[44] M. Marsman, J. Paier, A. Stroppa, and G. Kresse, J. Phys.: Condens. Matter **20**, 064201 (2008).
[45] S. L. Adler, Phys. Rev. **126**, 413 (1962).
[46] N. Wiser, Phys. Rev. **129**, 62 (1963).
[47] J. N. Plendl, L. C. Mansur, S. S. Mitra, and I. F. Chang, Solid State Commun. **7**, 109 (1969).
[48] P. J. Gielisse, J. N. Plendl, L. C. Mansur, R. Marshall, S. S. Mitra, R. Mykolajewycz, and A. Smakula, J. Appl. Phys. **36**, 2446 (1965).
[49] C. Rödl, F. Fuchs, J. Furthmüller, and F. Bechstedt, Phys. Rev. B **77**, 184408 (2008).
[50] F. Fuchs and F. Bechstedt, Phys. Rev. B **77**, 155107 (2008).
[51] R. Zimmermann, P. Steiner, R. Claessen, F. Reinert, S. Hüfner, P. Blaha, and P. Dufek, J. Phys.: Condens. Matter **11**, 1657 (1999).